

## 골판지 적층재와 EPS 사이의 압축거동에 대한 실험적 연구

### Experimental Study on Compression Behavior between Multi-layered Corrugated Structure and EPS Packaging Materials

박종민<sup>1\*</sup>, 최원식<sup>2</sup>, 김종순<sup>2</sup>

Jong-Min Park<sup>1\*</sup>, Won-Sik Choi<sup>2</sup>, Jong-Soon Kim<sup>2</sup>

#### 〈Abstract〉

The evaluation of the compression behavior of the cushioning material is of importance to achieve appropriate packaging design. In order to change packaging design from polymeric-based to more eco-friendly cellulose-based nire effectively, comparative study on the compression behavior between these two packaging materials is crucial. In this study, the stress-strain behavior, hysteresis loss, and response characteristics for cyclic loading were analyzed through compression tests on multi-layered corrugated structure (MLCS) and expanded polystyrene (EPS) packaging materials.

MLCS produced in Korea is produced by winding a certain number of single-faced corrugated paperboard, and the compression behavior of this material was turned out to be 6 stages: elastic stage, first buckling stage, sub-buckling stage, densification stage, last buckling stage and high densification stage. On the other hand, EPS's compression behavior was in 3 stages: linear elastic stage, collapse plateau, and densification stage. The strain energy per unit volume (strain energy density) of MLCS did not differ depending on the material thickness, but it showed a clear difference depending on the raw material and flute type. Hysteresis loss of MLCS ranged from 0.90 to 0.93, and there were no significant differences in the raw material and flute type. These values were about 5 to 20% greater than the hysteresis of the EPS (about 0.78 to 0.87).

*Keywords : Multi-layered corrugated paperboard, EPS, Compression behavior, Packaging, Stress-strain curve*

1\* 교신저자, 바이오산업기계공학과 교수, 부산대학교

E-mail: parkjssy@pusan.ac.kr

2 바이오산업기계공학과, 부산대학교

1\* Department of Bio-industrial Machinery Engineering Pusan National University, Korea

2 Department of Bio-industrial Machinery Engineering, Pusan National University, Korea

## 1. Introduction

Polymeric-based packaging materials, especially expanded polystyrene (EPS), have been mainly applied in packaging design of various products. However, as the environmental pollution caused by the generation of packaging waste has become a social problem, attempts to convert it to more eco-friendly cellulose-based materials have been tried.

Representative cellulose-based packaging materials used in Korea include multi-layered corrugated structure (MLCS) and pulp mold. Pulp molds are mainly suitable for the cushioning of lightweight products; however, they require metal mold. On the other hand, MLCS has a wide range of applications due to the high cushioning performance and compression strength of the corrugated paperboard itself. In addition, it does not require metal molds, so it has the advantage of not only shortening the product development period but also low-production cost on a volume basis and quick response to multi-item small sized production.

As shown in Fig. 1, MLCS is formed by winding a certain number of a single-faced corrugated paperboard (SFCP), utilizing high-energy absorption against the shock and vibration of corrugated flute. The designing parameter of MLCS are angle, channel, and flat type, and MLCS is produced in various forms by modifying each of them [1].

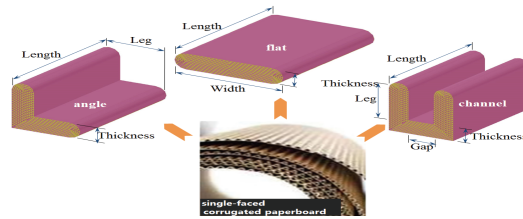


Fig. 1 Various products of MLCS

In order to develop eco-friendly packaging system, it is important to have a clear understanding of the difference in strength characteristics of EPS and MLCS packaging materials.

However, studies on compression comparison of MLCS with EPS have been rare. Most of MLCS studies attempted to analyze the effects of temperature and relative humidity on the cushioning performance and energy absorption properties of MLCS, and the effect of the flutes that make up it [2-4].

The purpose of this study was to quantitatively analyze the compression behavior of MLCS according to flute type, grade of raw material, and material thickness (number of layers of SFCP) in comparison with EPS packaging materials, and to analyze the effect of atmospheric conditions on these properties.

## 2. Material and Method

### 2.1 Materials

The raw materials (paperboards) of MLCS

used in this study were S120 and K180 manufactured by Korean old corrugated container (KOCC), and the flute types were A-flute (A/F) and B-flute (B/F).

In addition, the nominal thicknesses of the applied MLCS were 20, 30, 40, and 50 mm, and the number of layers of SFCP for each thickness is shown in Table 2. The size of the test piece was set to 15×15 cm.

Table 1. Specifications of SFCP used in the fabrication of MLCS

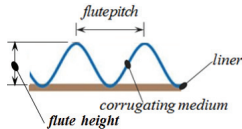
Raw material	Flute type	Specifications
S120	A/F	<ul style="list-style-type: none"> <li>height, wave length, and take-up-factor of flute: (A/F) 4.6mm, 8.8 mm, and 1.6; (B/F) 2.6mm, 6.0 mm, and 1.4</li> <li>thickness of paperboard: (K180) 0.24 mm; (S120) 0.19 mm</li> </ul> 
	B/F	
K180	A/F	
	B/F	

Table 2. Specifications of the MLCS used for the compression test

Raw material	Flute type	Nominal thickness, t							
		20 mm		30 mm		40 mm		50 mm	
		$t_a^{1)}$	$N^{2)}$	$t_a^{1)}$	$N^{2)}$	$t_a^{1)}$	$N^{2)}$	$t_a^{1)}$	$N^{2)}$
S120	A/F	17.0 (0.32)	4	27.5 (0.31)	6	37.0 (0.41)	8	48.3 (0.44)	10
	B/F	19.1 (0.24)	6	29.5 (0.27)	9	39.3 (0.27)	12	49.7 (0.38)	15
K180	A/F	18.8 (0.33)	4	28.1 (0.28)	6	37.7 (0.38)	8	48.7 (0.43)	10
	B/F	20.0 (0.21)	6	29.6 (0.25)	9	39.2 (0.23)	12	48.6 (0.30)	15

Note :1) actual thickness measured, ( ) standard deviation

2) the layer number of SFCP

In order to compare the compression behavior with MLCS, the density of EPS was 20 and 25 kg/m<sup>3</sup>. The test specimen of EPS was made to the same size as the test specimen of MLCS.

## 2.2 Experimental apparatus and method

The universal testing machine (UTM) used in this study is equipped with a load cell with a capacity of 1 ton (Fig. 2).

In the compression test, the loading rate was 12.5±2.5 mm/min [5], and the start of the compression displacement was set when the preload of 0.2 kgf was applied. Samples were equilibrated for more than 72 hr at each environmental condition (23°C-RH 50%, 23°C -RH 65%, 23°C-RH 80%) before the test [6].

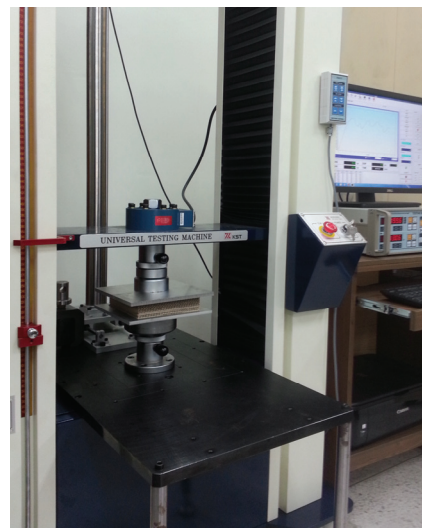


Fig. 2 The experimental apparatus for compression test

### 3. Result and Discussion

#### 3.1 Stress-strain (S-S) behavior

Unlike EPS, as shown in Fig. 3, the S-S curve of MLCS has several tops and belly parts, because several flutes making up MLCS are gradually collapsed during the flat compression test.

Wang and E [3] classified the S-S curve of MLCS into four stages: elastic stage, first buckling stage, sub-buckling stage, and densification stage. However, their MLCS sample was manufactured by stacking a number of single-wall corrugated paperboards, which is structurally different from the MLCS produced by wrapping a number of a SFCP as in this study.

In particular, MLCS made of SFCP doubles the basis weight and thickness of the central part because the flutes overlap each other in the first stage of production. Therefore, the compression process of MLCS used in this study can be divided into 6 stages (Fig. 3): elastic stage (A), first buckling stage (B), sub-buckling stage (C), densification stage (D), last buckling stage (E), and high densification stage (F). This process has two more steps than the compression process of MLCS proposed by Wang and E [3]. The 6 stages, however, can be largely compressed into 3 stages: the elastic stage (A), the plateau stage (B, C), and the densification stage (D, E).

The first buckling stage occurs when the

flutes that make up the MLCS first collapse. Subsequently, a continuous collapse of the flutes forms a plateau stage where the top and belly parts occur continuously. This stage continues until only one central hardened flute remains, eventually leading to a high densification stage where the load increases rapidly.

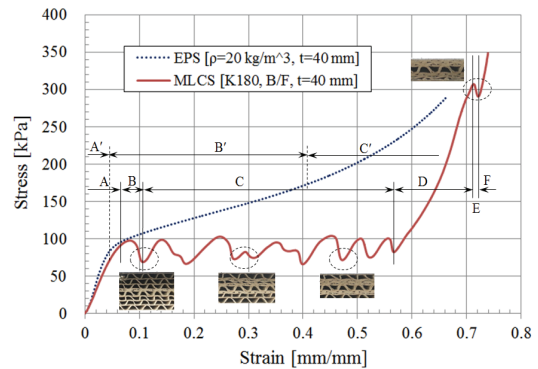


Fig. 3 Typical force-deformation curves of EPS and MLCS

As shown in Fig. 3, the S-S curve of EPS can be divided into three stages: linear elastic stage (A'), collapse plateau (B'), and densification stage (C'). The elastic stage (A') is governed by the bending of the cell wall in open-cell foam and the stretching of the cell wall in closed-cell foam. In the collapse stage (B'), the cells in the foam collapse due to the buckling of the cell wall, and in the densification stage (C'), the collapse and densification process continues and eventually reaches the bottom-out [7].

The area under the S-S curve represents the energy absorption per unit volume due to

the deformation of the material, that is, the strain energy density ( $\text{kJ}/\text{m}^3$ ).

Fig. 4 shows the S-S curves of MLCS and EPS under various conditions for a thickness of 40 mm, and Fig. 5 shows the force-deformation curves according to the specimen thickness of MLCS and EPS. Among the samples of MLCS, K180-B/F had the highest compressive resistance, followed by S120-B/F, K180-A/F, and S120-A/F. Similar trends were observed for thicknesses other than 40 mm.

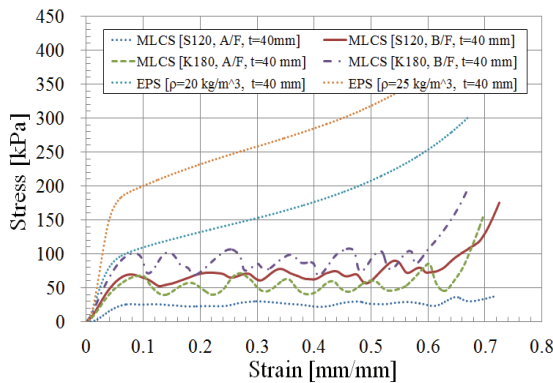


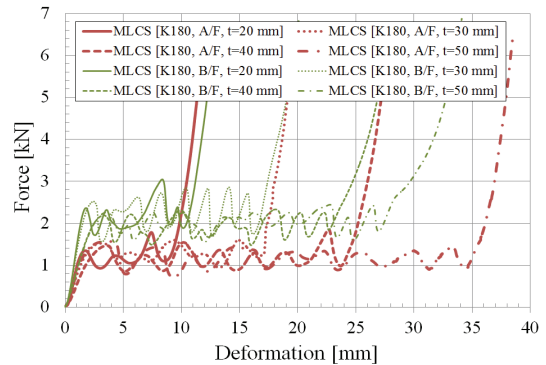
Fig. 4 The compression S-S curves of MLCS and EPS according to raw materials and flute type under standard condition (23°C-RH 50%)

The strain energy density ( $\text{kJ}/\text{m}^3$ ) according to the thickness of MLCS in the same raw material and flute type did not tend to be apparent (Table 3).

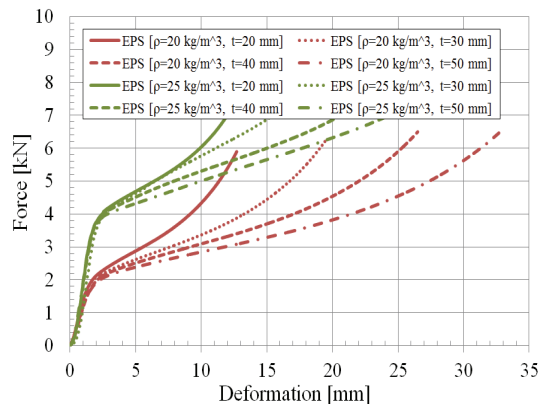
In contrast, in the case of EPS, the strain energy density slightly increased with the material thickness (Table 3). The strain energy density of EPS was about 1.2 to 9.5 times larger than MLCS of the same material thickness, and the difference was greatly

influenced by the raw material and flute type of MLCS.

In the paired t-tests of the raw material, flute type, and material thickness for the strain energy density of MLCS (Table 4), there were significant differences except the material thickness. EPS also showed significant differences in density. However, the material thickness didn't affect the strain energy density.



(a) MLCS\_K180



(b) EPS

Fig. 5 The compression force-deformation curves of MLCS\_K180 and EPS according to the material thickness under standard condition

### 3.2 Compressive resistance by environmental conditions

The energy absorption characteristic of MLCS against external forces are influenced by relative humidity [3].

When compressing the MLCS specimen to 2/3 of each material thickness, the strain energy densities in different relative humidities are

shown Table 3. The strain energy density of MLCS decreased significantly with increasing relative humidity. Within the relative humidity range of this study, the B/F-K180 showed the highest value, followed by B/F-S120, A/F-K180, and A/F-S120.

The strain energy density decreases as the relative humidity increases, because the moisture content increases as well; increasing

Table 3. Compressive strain energy density and hysteresis loss of MLCS and EPS under various conditions

Classify		t (mm)	Strain energy density <sup>1)</sup> (kJ/m <sup>3</sup> )			Energy <sup>2)</sup> (kJ/m <sup>3</sup> )		
			rh 50%	rh 65%	rh 80%	loading E	unloading E	hysteresis loss
MLCS S120	A/F	20	16.9(1.4)	16.4(1.5)	14.2(1.4)	11.5(2.1)	1.1(0.1)	0.90(0.04)
		30	16.1(2.3)	15.1(2.1)	12.3(2.1)	10.8(2.0)	1.1(0.1)	0.89(0.07)
		40	16.1(1.2)	15.3(1.2)	11.9(1.4)	11.7(2.1)	0.9(0.1)	0.92(0.06)
		50	17.5(1.7)	16.8(1.6)	13.8(1.4)	12.8(3.1)	1.1(0.1)	0.91(0.06)
	B/F	20	51.3(3.1)	49.0(3.0)	43.9(2.9)	30.5(4.0)	2.1(0.1)	0.93(0.08)
		30	39.7(4.4)	37.9(3.8)	31.2(3.0)	30.9(4.1)	2.7(0.2)	0.91(0.06)
		40	43.4(3.8)	38.8(3.5)	31.8(3.0)	30.3(4.2)	2.0(0.2)	0.93(0.06)
		50	43.0(4.0)	37.3(4.1)	30.4(3.9)	29.3(3.9)	2.0(0.1)	0.93(0.07)
MLCS K180	A/F	20	57.1(5.2)	48.0(5.0)	37.6(5.0)	28.2(4.0)	2.3(0.1)	0.92(0.08)
		30	44.2(3.6)	41.4(3.0)	29.7(3.0)	26.1(2.9)	1.7(0.1)	0.94(0.09)
		40	34.0(3.2)	30.6(3.0)	29.6(3.1)	25.6(3.3)	1.8(0.2)	0.93(0.04)
		50	37.5(3.0)	31.7(2.9)	30.3(3.1)	26.2(3.8)	1.8(0.2)	0.93(0.06)
	B/F	20	77.0(5.2)	57.3(4.9)	52.8(5.0)	40.0(4.0)	3.7(0.2)	0.91(0.08)
		30	72.5(4.3)	63.6(5.1)	55.6(5.0)	46.0(5.5)	3.5(0.3)	0.92(0.06)
		40	59.1(4.0)	58.2(4.9)	50.4(5.2)	43.2(5.0)	3.0(0.2)	0.93(0.07)
		50	64.0(5.0)	56.3(4.9)	48.4(4.8)	42.1(4.3)	2.9(0.3)	0.93(0.06)
EPS $\rho=20$ kg/m <sup>3</sup>	20	97.0(3.4)	—	—	62.7(3.4)	13.3(1.5)	0.79(0.02)	
	30	103.5(4.1)	—	—	63.8(3.4)	12.8(1.6)	0.80(0.04)	
	40	107.2(4.0)	—	—	68.7(3.9)	12.3(1.9)	0.82(0.02)	
	50	107.6(4.1)	—	—	71.6(4.0)	11.5(1.4)	0.84(0.02)	
EPS $\rho=25$ kg/m <sup>3</sup>	20	117.4(5.0)	—	—	87.1(3.9)	15.3(2.1)	0.82(0.03)	
	30	153.3(5.0)	—	—	93.1(4.0)	14.9(2.0)	0.84(0.03)	
	40	158.1(5.4)	—	—	105.3(4.1)	14.6(1.4)	0.86(0.02)	
	50	161.6(6.3)	—	—	115.9(5.0)	14.3(1.7)	0.88(0.03)	

Note : ( ) standard deviation

Table 4. Mean comparison by Duncan's multiple range tests for strain energy density and hysteresis loss of MLCS

MLCS				
Variety	Raw material	Flute type	Material thickness	Relative humidity
Strain energy density	S120 <sup>a</sup> , K180 <sup>b</sup>	A/F <sup>a</sup> , B/F <sup>b</sup>	20 <sup>a</sup> , 30 <sup>a</sup> , 40 <sup>a</sup> , 50 <sup>a</sup>	50 <sup>a</sup> , 65 <sup>b</sup> , 80 <sup>c</sup>
Hysteresis loss	S120 <sup>a</sup> , K180 <sup>a</sup>	A/F <sup>a</sup> , B/F <sup>a</sup>	20 <sup>a</sup> , 30 <sup>a</sup> , 40 <sup>a</sup> , 50 <sup>a</sup>	no
EPS				
Variety	Density	Material thickness		
Strain energy density	20 <sup>a</sup> , 25 <sup>b</sup>	20 <sup>a</sup> , 30 <sup>a</sup> , 40 <sup>a</sup> , 50 <sup>a</sup>		
Hysteresis loss	20 <sup>a</sup> , 25 <sup>a</sup>	20 <sup>a</sup> , 30 <sup>a</sup> , 40 <sup>b</sup> , 50 <sup>b</sup>		

Note : a,b,c letters indicate the statistical difference in rows (significant level at 5%).

the the water molecules attached to the fibers weakens the chemical bonding strength of the fibers and ultimately leads to the deterioration of the physical properties. Based on the ANOVA test the relative humidity had a significant effect on the strain energy density of MLCS in Table 4 ( $P < 0.05$ ) [8].

Compared to the strain energy density of EPS ( $\rho=20 \text{ kg/m}^3$ ,  $t=40 \text{ mm}$ ) measured at 50% relative humidity, the strain energy density of S120-A/F, S120-B/F, K180-A/F, and K180-B/F was about 15%, 40%, 32%, and 55% levels, respectively. This difference could be greater when the relative humidity is higher because the MLCS is sensitive to the relative humidity.

Considering that the EPS softens with increasing temperature and the MLCS becomes a more rigid structure, the difference in strain energy between the EPS and MLCS is expected to decrease significantly at higher temperatures [9, 10]. Therefore, it is necessary to consider the

temperature and humidity conditions when selecting the cushioning material in the packaging design.

### 3.3 Response for cyclic loading

Fig. 6 shows the responses of MLCS and EPS to cyclic loading, which repeat the process of compressing the specimen to 62.5% of the thickness of each specimen at a constant speed ( $12.5 \pm 2.5 \text{ mm/min}$ ) and then removing it.

MLCS was elastic after the plateau stage where its constituent flutes collapse in succession. The corrugated flute exhibits a high stiffness when it acts as a structural element at the time of the initial force; when it exceeds the buckling strength, the flute undergoes a significant plastic deformation, collapsing the flutes. As a results, it becomes elastic.



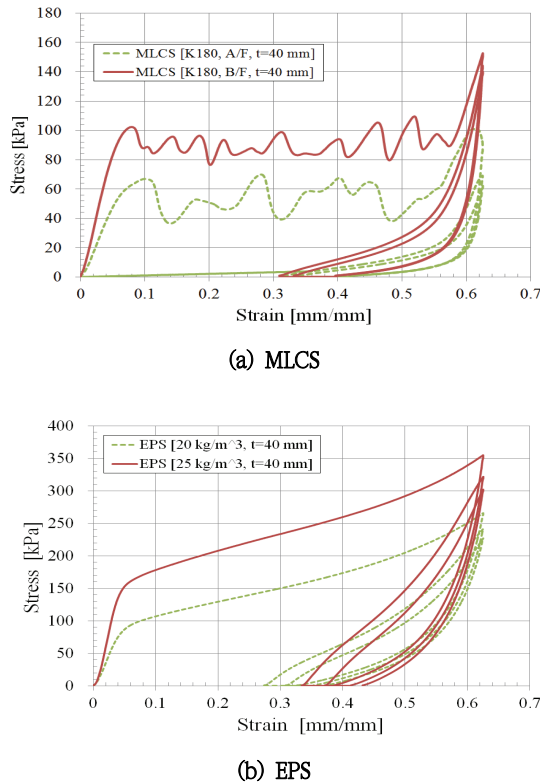


Fig. 6 The compression S-S curves of MLCS and EPS for cyclic loading

Sek et al. [11] reported the possibility of developing a composite cushioning system that can extend the scope of protection against drops and impacts by taking advantage of this inherent dual behavior of MLCS. The primary element of this composite cushioning system is an elastic deformation mode to provide cushioning for frequently occurring small impacts, and the secondary element is a plastic deformation mode designed to absorb impact energy caused by sudden impacts and drops.

The area of the closed section on the

loading-unloading curve appearing after one cyclic loading of the specimen represents the amount of work lost during the process, and the ratio of this value to the total energy applied to the specimen under load is the hysteresis loss.

Only the data corresponding to one cyclic loading was extracted from the data shown in Fig. 6, and the loading energy, unloading energy, and hysteretic loss were analyzed. In the case of MLCS, unlike the material thickness, there was significant difference in values with raw material and flute type.

The hysteresis loss of MLCS ranged from 0.90 to 0.93; thus, the difference of these values among raw material and flute type was negligible. Hysteresis loss of EPS increased with the material thickness. The value ranged from approximately 0.78 to 0.87, which was 84-97% of MLCS.

In paired t-tests by raw material, flute type, and material thickness for the hysteresis of MLCS shown in Table 3; the differences were not statistically insignificant. EPS was also analyzed to be insignificant depending on density and material thickness [8].

## 4. Conclusion

In order to accelerate the conversion of the conventional polymeric-based cushioning system to a more eco-friendly cellulose-based cushioning system, it is important to have an clear understanding of the difference



in strength characteristics of EPS and MLCS packaging materials.

The compression characteristics of MLCS and EPS packaging materials, which are commonly used in Korea, were compared and analyzed in various ways by experimental methods. The results are summarized as follows.

- (1) Compression behavior of MLCS produced by laminating SFCP was divided into 6 stages: elastic stage, first buckling stage, sub-buckling stage, densification stage, last buckling stage, and high densification stage.
- (2) The strain energy density of MLCS was different with the raw material and flute type. In addition, the strain energy density decreased with the relative humidity.
- (3) Hysteresis loss of MLCS ranged from 0.90 to 0.93 with very little difference in the raw material and flute type. Compared to the hysteresis of EPS (about 0.78-0.87), hysteresis loss at MLCS was about 5 to 20% larger.

## References

- [1] J. M. Park and J. G. Han, Transport packaging design engineering, Munundang, (2011).
- [2] D. Wang, "Cushioning properties of multi-layer corrugated sandwich structures," *Journal of Sandwich Structures and Materials*, vol. 11, no. 1, pp. 57~66, (2009).
- [3] Z. W. Wang, and Y. P. E, "Energy absorption properties of multi-layered corrugated paperboard in various ambient humidities," *Material and Design*, vol. 32, no. 6, pp. 3476~3485, (2011).
- [4] D. Wang, H. Gong, and Z. Bai, "Effect investigation of relative humidity and temperature on multi-layer corrugated sandwich structures," *Journal of Sandwich Structures and Materials*, vol. 15, no. 2, pp. 156~167, (2013).
- [5] ISO 3035, Single-faced and single-wall corrugated fibreboard-determination of flat crush resistance.
- [6] ISO 187, Paper, board and pulps - Standard atmosphere for conditioning and testing and procedure for monitoring the atmosphere and conditioning of samples.
- [7] D. Eaves, "Handbook of polymer foams," Shropshire, UK: Rapra Technology Limited.
- [8] R Development Core Team, R: A language and environment for statistical computing, R Foundation for Statistical Computing, Vienna, Austria, (2011).
- [9] J. Marcondes, "Cushioning properties of corrugated fiberboard and the effects of moisture content," *Transactions of the ASAE*, vol. 35, no. 6, pp. 1949~1953, (1992).
- [10] J. Marcondes, K. Hatton, J. Graham, and H. Schueneman, "Effect of temperature on the cushioning properties of some foamed plastic materials," *Packaging Technology and Science*, vol. 16, no. 2, pp. 69~76, (2003).
- [11] M. Sek, V. Rouillard, H. Tarash, and S. Crawford, "Enhancement of cushioning performance with paperboard crumple inserts," *Packaging Technology and Science*, vol. 18, no. 5, pp. 273~278, (2005).